Title
POTENTIAL CURVES AND INELASTIC CROSS SECTIONS FOR LOW ENERGY COLLISIONS OF O+ AND He

Author
Schaefer, H.F.

Publication Date
1972-12-01

Submitted to
Journal of Chemical Physics

LBL-1187
Preprint

POTENTIAL CURVES AND INELASTIC CROSS SECTIONS FOR LOW ENERGY COLLISIONS OF O^+ AND He

S. D. Augustin, W. H. Miller,
P. K. Pearson, and H. F. Schaefer III

December 1972

Prepared for the U. S. Atomic Energy
Commission under Contract W-7405-ENG-48

DISCLAIMER

POTENTIAL CURVES AND INELASTIC CROSS SECTIONS FOR LOW ENERGY COLLISIONS OF O^+ AND He^+

by

S. D. Augustin, W. H. Miller

Inorganic Materials Research Division, Lawrence Berkeley Laboratory and Department of Chemistry; University of California, Berkeley, California 94720

and

P. K. Pearson and H. F. Schaefer III*

Nuclear Chemistry Division, Lawrence Berkeley Laboratory and Department of Chemistry; University of California, Berkeley California 94720

ABSTRACT

Potential curves corresponding to all the valence states of HeO^+ have been calculated with a minimum basis set and full configuration interaction. The principal inelastic process in low energy collisions of ground state He and O^+ is seen to be the $^4S \rightarrow {}^2D$ excitation of O^+, the transition arising from a spin-orbit interaction at a crossing of the lowest $^4\Sigma$ and $^2\Pi$ states of HeO^+. Much more accurate calculations were thus carried out for these two states, as well as a semiclassical calculation of the cross section for $He + O^+(^4S) \rightarrow He + O^+(^2D)$. The cross section has no activation energy other than its energetic threshold (3.3 eV) and rises to a maximum of $\sim 8.6 \times 10^{-3}$ $\mathring{A}^2$ at $\sim$ 6 eV. There is

a residual oscillatory structure in the energy dependence of the cross section, and it is shown how experimental observation of this could be used to obtain precise information concerning the relevant potential curves.

I. Introduction

To the extent that one can determine reliable potential energy curves for the low-lying electronic states of diatomic molecules, the problem of electronic transitions in low energy atom-atom collisions is to a large degree a solved problem. The reason for this is that at low collision energies (~ 10 eV, say) curve-crossings effectively dominate the picture (i.e., a particular transition has an appreciable cross section only if it can take place via a curve crossing), and the two-state atom-atom curve-crossing problem was essentially solved 40 years ago by Landau, Zener and Stuckelberg[1-4].

This paper reports calculations of the electronic potential curves that correspond to valence states of the HeO^+ system, i.e., all the diatomic potential curves that arise from the ground states of He and He^+, the ^4S_u, ^2D_u, and ^2P_u states of O^+, and the ^3P_g, ^1D_g, and ^1S_g states of O. Section II describes these calculations and discusses a number of qualitative predictions that can be made about the low energy collision processes simply by examining the potential curves themselves.

The principal inelastic process at low energy appears to be

$$He(^1S) + O^+(^4S_u) \rightarrow He(^1S) + O^+(^2D_u) \quad , \qquad (1)$$

the relevant potential curves being coupled by a spin-orbit interaction. Section III thus presents a calculation of this inelastic cross section as a function of initial collision energy; there is no activation energy necessary for the transition, the cross section rising from its threshold at 3.3 eV to a maximum of ~ 8.6×10^{-3} $\mathring{A}^2$ at ~ 6 eV and then falling off slowly at higher energy in the typical Landau-Zener fashion. There is a

residual oscillatory structure in the energy dependence of the cross section, and Section III shows how observation of this could be used to determine precise information about the lowest $^4\Sigma$ and $^2\Pi$ poential curves.

II. Potential Curves

A. Method of Calculation.

The total energy as a function of internuclear separation was calculated with a configuration interaction computer program[5], thus including electron correlation in the wavefunctions. Two sets of potential curve calculations were carried out: first, a set of minimum basis full CI calculations on several states provided a rough picture of the system; then, far more elaborate calculations were performed on a few states which seemed interesting in the simpler calculations.

The minimum basis calculations included 13 of the 14 states arising from the 6 lowest states of the separated atoms (3 states for separated He and O^+, 3 for separated He^+ and O). The basis set included, on oxygen: 1s (ζ = 7.655), 2s (ζ = 2.295), 2p (ζ = 2.317); on helium: 1s (ζ = 1.840). The orbital exponents are averages of the corresponding optimized ζ's for the atoms and the ions, an admittedly crude procedure, but presumable adequate for the rough picture desired. Because of the small basis set, the calculated wavefunctions were constructed from very few configurations, the exact number ranging from 4 to 24. These preliminary full CI calculations are analogous to those carried out by Schaefer and Harris[6] for the oxygen molecule.

The more elaborate calculations used a basis set of 6s, 4p, and 1d

Slater functions on oxygen, 3s and 2p-type orbitals on helium, contracted into 14σ and 6σ molecular orbitals, as shown in Table I. The $^4\Sigma^-$, $^2\Pi$, and $^4\Pi$ states were studied with this basis set.

Since full configuration interaction calculations with this many orbitals would have required a formidable number of configurations in the wavefunction, we restricted ourselves to "first-order" wavefunctions[7], composed of restricted sets of configurations. The configurations included in a first-order wavefunction are:

i) all configurations in which only valence orbitals are occupied (1σ, 2σ, 3σ, 4σ and 1π in this case), and

ii) all single excitations from the configurations in part i).

For a further reduction in the number of configurations, we restricted the 1σ orbital to be doubly occupied except for single excitations from the reference configuration. (In the case of the $^2\Pi$ state, there are two reference configurations[8], namely $1\sigma^2 2\sigma^2 3\sigma^2 1\pi^3$ and $1\sigma^2 2\sigma^2 3\sigma^2 4\sigma^2 1\pi$. All singles from both were included.) Configurations in the $^4\Sigma^-$ first-order wavefunction are tabulated in Table II. For the $^4\Sigma^-$ state 209 configuration were included, for $^2\Pi$ 417, and for $^4\Pi$ 265.

Each calculation began with a self-consistent-field (SCF) stage to provide reasonable starting orbitals for the later first-order state. SCF orbitals were obtained by performing natural-orbital iterations on the wavefunction composed of the reference configuration(s) and all single excitations therefrom. In the $^4\Sigma^-$ and $^4\Pi$ cases, a short HeO^{++} calculation followed the SCF stage to rotate the SCF orbitals into a consistent order.[9] Finally, natural orbital interations[10] were performed on the first-order

wavefunction until the energy improvement from one iteration to the next fell below a threshold of 10^{-5} hartree. The resultant energies are presented in Table III.

B. Qualitative Observations.

Figure 1 shows the potential curves for all the valence states of HeO^+ (suitably shifted vertically so that the dissociation limits correspond to the experimental atomic energy levels[11]). Simply inspecting them leads to a number of qualitative predictions concerning the possible low energy collision processes.

(1) For collisions of the He with ground state $O^+(^4S)$ the principal inelastic transition should be excitation of the ^2D state of O^+,

$$He + O^+(^4S) \rightarrow He + O^+(^2D) \quad . \qquad (2)$$

Since the relevant crossing of the $^4\Sigma$ and $^2\Pi$ states occurs just below the asymptotic limit of the $^2\Pi$ curve, there should be no activation energy for this transition (other than the 3.3 eV threshold energy itself).

(2) The ^2D state of O^+ should be readily quenched by collision with He, the inverse transition of Equation (2), whereas the ^2P state should not be.

(3) Low energy collisions of He^+ with ground state $O(^3P)$ should lead to charge transfer exclusively into the ^2P state of O^+,

$$He^+ + O(^3P) \rightarrow He + O^+(^2P) \quad , \qquad (3)$$

and there should be little if any activation energy for this transition.

(4) The ^1D state of O should be readily deactivated by He^+ to ground state O,

$$He^+ + O(^1D) \rightarrow He^+ + O(^3P) \quad . \tag{4}$$

(5) The ^1S state of O, on the other hand, should be quenched by He^+ only via a charge transfer process leading exclusively to the ^4P state of O^+ (of the valence-excited configuration $2s2p^4$),

$$He^+ + O(^1S) \rightarrow He + O^+(^4P). \tag{5}$$

III. INELASTIC CROSS SECTIONS.

This section discusses the calculation of the inelastic transition related to the crossing of the lowest $^2\Pi$ and $^4\Sigma$ potential curves, i.e., Equation (2). The semiclassical Landau-Zener-Stuckelberg (LZS) Theory[1-4] is ideally suited for this curve crossing problem, the only tricky aspect of the calculation being the determination of the spin-orbit coupling at the crossing point. First we summarize the appropriate cross section formulae, then estimate the spin-orbit coupling, and finally present the results of the cross section for the transition in Equation (1).

A. Summary of LZS Expressions.

The cross section for the $1 \rightarrow 2$ electronic transition is given by

$$\sigma_{2 \leftarrow 1}(E_1) = 2\pi \int_0^\infty db\, b\, P_{2 \leftarrow 1}(b,E_1) \quad , \tag{6}$$

where $P_{2 \leftarrow 1}(b,E_1)$ is the transition probability as a function of impact parameter b and initial translational energy E_1. If the transition is dominated by a single, well-defined curve-crossing, then the LZS approximation gives the transition probability as

$$P_{2 \leftarrow 1} = e^{-2\delta}(1 - e^{-2\delta})\, 4\pi z^{1/2} Ai^2(-z) \quad . \tag{7}$$

In Equation (7) δ is the imaginary part of a classical action integral

$$2\delta = \mathrm{Im} \int_{r_-}^{r_+} dr\, [k_2(r) - k_1(r)] \quad , \tag{8}$$

where $k_2(r)$ and $k_1(r)$ are the local momenta on the adiabatic, or diagonalized potential curves

$$k_i(r) = \{2\mu[E - W_i(r) - E_1 b^2/r^2]\}^{1/2}/\hbar \quad , \tag{9}$$

and $r_\pm$ are the two complex crossing points of the adiabatic potentials, i.e., the roots of the equation.

$$W_1(r) = W_2(r) \quad ; \tag{10}$$

r_+ and r_- are complex conjugates. The adiabatic potentials $W_i(r)$ are the eigenvalues of the 2-by-2 matrix

$$\begin{matrix} V_1(r) & V_{12}(r) \\ V_{12}(r) & V_2(r) \end{matrix} \quad , \tag{11}$$

where $V_i(r)$ are the $^4\Sigma$ and $^2\Pi$ potential curves and $V_{12}(r)$ is the spin-orbit coupling between these two states. [An illustration of the confusion in the language related to the curve-crossing problem is the fact that the Born-Oppenheimer $^4\Sigma$ and $^2\Pi$ potential curves, which are ordinarily referred to as "adiabatic" curves, are in this case the "diabatic" curves which actually cross.]

The variable z in Equation (7) is related to the difference of the classical action integrals on the potentials $W_i(r)$ from their respective classical turning points to the crossing point:

$$z = (3/2\ \tau)^{2/3} \quad , \tag{12}$$

where

$$\tau = \int_{r_1}^{r_o} dr\, k_1(r) - \int_{r_2}^{r_o} dr\, k_2(r) \quad , \tag{13}$$

with $r_o = \mathrm{Re}(r_\pm)$. The usual form of Equation (7) [cf. Stuckelberg[3]] corresponds to use of the asymptotic form of the Airy function, whereby

$$4\pi z^{1/2}\, \mathrm{Ai}^2(-z) \to 4 \sin^2(\tfrac{\pi}{4} + \tau) \quad ; \tag{14}$$

use of the Airy function form in Equation (7) makes the expression applicable even for small τ (i.e., when the crossing point is close to the turning points) where the usual result is invalid.

For the present application it is not necessary to employ Equation (7) in its full generality as summarized above. Since the spin-orbit interaction is so weak ($\sim 10^{-2}$ eV), for example, Equation (8) effectively reduces to the usual Landau-Zenar approximation

$$2\delta \simeq \frac{2\pi}{\hbar v_o} \frac{|V_{12}(r_o)|^2}{|V_1'(r_o) - V_2'(r_o)|} \quad , \tag{15}$$

where $V_{12}(r_o)$ is the spin-orbit coupling and v_o the velocity at the crossing point r_o, the value of r for which $V_1(r) = V_2(r)$. Similarly, the action integrals in [Equation (13)] can be evaluated using the potential curves $V_i(r)$; i.e., $W_1(r)$ [$W_2(r)$] can be replaced by $V_2(r)$ [$V_1(r)$] in Equation (9). It should be noted, however, that this Landau-Zener approximation to Equation (8) is valid only because of the very weak coupling, and it would typically not be valid for a strongly "avoided intersection" of two Born-Oppenheimer potential curves of the same symmetry.

Although the Landau-Zener approximation in Equation (15) is valid in the present case (as was verified computationally), the other Landau-Zener approximation indicated by Equation (14) causes a noticeable change in the magnitude of the calculated cross section. The reason for this is that the weakness of the spin-orbit interaction causes the most significant impact parameters to be those for which the crossing point is close to the turning points - precisely the situation for which the approximation in Equation (14) is poorest.

B. Estimation of the Spin-Orbit Coupling.

A rigorous calculation of the spin-orbit coupling between the two molecular states would be a substantial project in itself[12], but a reasonable estimate can be made quite easily[13] by using information from atomic spin-orbit interactions.

Quite briefly, one assumes the molecular spin-orbit Hamiltonian to be a sum of terms related to each of the nuclei separetely,

$$H_{so} = \sum_{i,N} \xi_N(r_{iN})\ \vec{\ell}_i \cdot \vec{s}_i \quad , \tag{16}$$

where r_{iN} is the distance from electron i to nucleus N, and for purposes of estimating the matrix element of this operator one writes the wavefunctions in terms of individual atomic states. Our $^4\Sigma$ wavefunction at the crossing point, for example, had one dominant configuration, corresponding to the ground state of He and the ^4S state of O^+,

$$|\,^4\Sigma\,>_{HeO^+} \simeq |\,^1S\,>_{He} |\,^4S_{3/2}\,>_{O^+} \quad . \tag{17}$$

The $^2\Pi$ state, on the other hand, involves three significant atomic

components at the crossing point,

$$|^2\Pi>_{HeO^+} \quad 0.631|^1S>_{He}|^2P_{3/2}>_{O^+} + 0.668|^1S>_{He}|^2D_{5/2}>_{O^+}$$

$$- 0.338|^1S>_{He}|^2D_{3/2}>_{O^+} \quad . \tag{18}$$

In constructing the matrix element of the spin-orbit operator between these two wavefunctions one furthermore neglects overlap between orbitals centered on different nuclei. Since all the wavefunctions contain only the ^1S state of He, there is no contribution to the spin-orbit coupling related to this center, and one thus obtains

$$V_{12} \equiv <^2\Pi|H_{so}|^4\Sigma> \simeq 0.631 < ^2P_{3/2}|H_{so}^{O^+}|^4S_{3/2}>$$

$$+ 0.668 < ^2D_{5/2}|H_{so}^{O^+}|^4S_{3/2}> - 0.338 < ^2D_{3/2}|H_{so}^{O^+}|^4S_{3/2}> ,$$

where $H_{so}^{O^+}$ is the atomic spin-orbit operator for O^+ alone. The atomic spin-orbit interaction between ^4S and ^2D states of O^+ is zero, however, so that this becomes

$$V_{12} \simeq 0.631 < ^2P_{3/2}|H_{so}^{O^+}|^4S_{3/2}> \quad . \tag{19}$$

The spin-orbit matrix element connecting $^2P_{3/2}$ and $^4S_{3/2}$ states of the $2p^3$ configuration is equal to ζ , the 2p radial integral of the effective central force interaction[14],

$$\zeta \equiv \int_0^\infty dr\, r^2\, 2p(r)^2\, \xi_{O^+}(r) \quad .$$

In most cases it is possible to determine the value of ζ from the atomic spin-orbit splittings, but for the $2p^3$ configuration the first order spin-orbit splittings vanish[14]. By noting, however, that the ζ values

for $O^{+3}(2p^1)$, $O^{+2}(2p^2)$, and $O(2p^4)$ are 256 cm^{-1}, 202 cm^{-1}, and 153 cm^{-1}, respectively, one can interpolate and obtain a value of 168 cm^{-1} for $O^{+}(2p^3)$. The spin-orbit interaction connecting the $^4\Sigma$ and $^2\Pi$ states at the crossing point is thus estimated to be

$$V_{12} \simeq (0.631)(168\ cm^{-1}) = 106\ cm^{-1} \quad , \tag{20}$$

which should be reliable to within 20% or so.

C. Results.

Figure 2 shows the cross section for the $^4S \rightarrow {}^2D$ excitation of O^+ as a function of initial collision energy, as calculated from Equations (6)-(7), with z and δ given by Equations (12)-(13) and (15), respectively; as noted in Section IIIA, there is no loss of accuracy for the present application in using this Landau-Zener approximation for δ. If the additional approximation in Equation (14) is made, however, the results in Figure 2 are increased uniformly by ~ 20%.

The oscillatory structure in the cross section in Figure 2 is a remnant of the oscillatory nature of $P_{2 \leftarrow 1}(b,E_1)$. Thus if the approximation in Equation (14) is made, and one in addition replaces $\sin^2(\frac{\pi}{4} + \tau)$ by 1/2 - i.e.,

$$4\pi z^{1/2}\, Ai^2(-z) \rightarrow 2$$

- the oscillations in $\sigma_{2 \leftarrow 1}$ versus E_1 disappear.

To understand the nature of this oscillatory structure in the energy dependence of the cross section the following analysis is useful. With the approximation in Equation (14) the cross section is given by

$$\sigma_{2\leftarrow 1}(E_1) = 2\pi \int_0^\infty db\ b\ \bar{P}_{2\leftarrow 1}(b,E_1)\ 2\ \sin^2[\tfrac{\pi}{4} + \tau(b)] \quad , \tag{21}$$

where

$$\bar{P}_{2\leftarrow 1}(b,E_1) = 2\ e^{-2\delta}(1 - e^{-2\delta})$$

is the phase averaged transition probability.

Since

$$2\ \sin^2[\tfrac{\pi}{4} + \tau(b)] = 1 + \sin[2\tau(b)] \quad ,$$

Equation (21) becomes

$$\sigma_{2\leftarrow 1}(E_1) = \bar{\sigma}(E_1) + \Delta\sigma(E_1) \quad , \tag{22}$$

where the non-oscillatory part of the cross section is the usual Landau-Zener result

$$\bar{\sigma}(E_1) = 2\pi \int_0^\infty db\ b\ \bar{P}_{2\leftarrow 1}(b,E_1) \quad ,$$

and the oscillatory part is given by

$$\Delta\sigma(E_1) = 2\pi \int_0^\infty db\ b\ \bar{P}_{2\leftarrow 1}(b,E_1)\ \sin[2\tau(b)] \quad . \tag{23}$$

For purposes of estimating $\Delta\sigma(E_1)$ the introduction of the approximation in Equation (14) is not too serious, for the dominant region of b that contributes to the integral in Equation (23) is $b \sim 0$ where $\tau(b)$ is large and Equation (14) valid. Expanding the integrand of Equation (23) about $b = 0$,

$$\Delta\sigma(E_1) \simeq 2\pi \int_0^\infty db\ b\ \bar{P}_{2\leftarrow 1}(0,E_1)\ \sin[2\tau(0) + 2b\tau'(0)] \quad ,$$

gives the desired result:

$$\Delta\sigma(E_1) = -\frac{\pi}{2}\,\bar{P}_{2\leftarrow 1}(0,E_1)[\tau'(0)]^{-2}\sin[2\tau(0)] \quad . \tag{24}$$

Equation (24) does not predict the magnitude of the oscillations in $\sigma_{2\leftarrow 1}(E_1)$ particularly well, but it describes the frequency of the oscillations in Figure 2 essentially exactly. Observation of these oscillations in the energy dependence of the cross section would thus determine the energy dependence of τ at zero impact parameter; i.e., $\tau_o(E)$, which is given by

$$\tau_o(E) = \int_{r_2}^{r_o} dr\,\{2\mu[E - V_2(r)]/\hbar^2\}^{1/2} - \int_{r_1}^{r_o} dr\,\{2\mu[E - V_1(r)]/\hbar^2\}^{1/2} \quad , \tag{25}$$

would be an experimentally known function. An RKR-like integral transform of this function could thus be used to give definite information about the crossing potential curves. Proceeding in the usual fashion[15], one obtains the following result:

$$r_1(E) - r_2(E) = r_1(0) - r_2(0) + \frac{2}{\pi}\left(\frac{\hbar^2}{2\mu}\right)^{1/2}\int_0^E dE'\,\tau_o'(E')(E - E')^{-1/2} \quad , \tag{26}$$

$r_1(E)$ and $r_2(E)$ being the classical turning points for b = 0 and energy E on potential curves $V_1(r)$ and $V_2(r)$, respectively. Equation (26) pertains as written to the case that the position of the crossing point is below $V_2(\infty)$, the asymptotic value of the excited state. If the crossing point is above this value, then the result becomes

$$r_1(E) - r_2(E) = \frac{2}{\pi}\left(\frac{\hbar^2}{2\mu}\right)^{1/2} \int_{V_o}^{E} dE' \, \tau_o'(E')(E - E')^{-1/2} \quad , \qquad (26')$$

V_o being the common value of V_1 and V_2 at the crossing point.

Observation of oscillatory structure in $\sigma_{2 \leftarrow 1}(E_1)$ would thus be a valuable piece of information in obtaining precise knowledge about the potential curves involved in the transition. Equations (26) and (26') show specifically what this information is, namely the lateral distance between points on the potential curves $V_1(r)$ and $V_2(r)$ that correspond to the same value of the total energy.

† This research has been supported by the United States Atomic Energy Commission under contract W-7405-eng-48 and in part by the Petroleum Research Fund, administered by the American Chemical Society.

* Alfred P. Sloan Fellow.

1. L. Landau, Phys. Z. Sowjetunion 1, 46 (1932).
2. C. Zener, Proc. Roy. Soc. (London) A 137, 696 (1932).
3. E. C. G. Stuckelberg, Helv. Phys. Acta 5, 369 (1932).
4. See also more recent work by (a) V. Bykhovskii, E. E. Nikitin, and M. Ya. Ovchinnkova, JETP 20, 500 (1965), and (b) W. R. Thorson, J. B. Delos, and S. A. Boorstein, Phys. Rev. A 4, 1052 (1971).
5. H. F. Schaefer, J. Comput. Phys. 6, 142 (1970); J. Chem. Phys. 52, 6241 (1970).
6. H. F. Schaefer and F. E. Harris, J. Chem. Phys. 48, 4946 (1968).
7. H. F. Schaefer, J. Chem. Phys. 54, 2207 (1971).
8. Two reference configurations were required for the $^2\Pi$ calculations since the restricted Hartree-Fock wave function does not dissociate to ^1S He plus ^2D O^+ Hartree-Fock wave functions. Inclusion of the $1\sigma^2 2\sigma^2 3\sigma^2 4\sigma^2 1\pi$ configuration allows proper dissociation.
9. C. F. Bender and H. F. Schaefer, J. Chem. Phys. 55, 4798 (1971).
10. C. F. Bender and E. R. Davidson, J. Phys. Chem. 70, 2675 (1967).
11. C. E. Moore, Atomic Energy Levels, Cir. No. 467, Nat. Bureau Stds., Washington, D.C., 1949.
12. R. H. Pritchard and C. W. Kern, J. Chem. Phys. 57, 2590 (1972).
13. See, for example, (a) H. Lefebvre-Brion and C. M. Moser, J. Chem.

Phys. 44, 2951 (1966); and (b) R. L. Ellis, R. Squire and H. H. Jaffe, J. Chem. Phys. 55, 3499 (1971).

14. E. U. Condon and G. H. Shortley, The Theory of Atomic Spectra, Cambridge U.P., 1963, pp. 266 et seq.

15. See, for example, W. H. Miller, J. Chem. Phys. 54, 4174 (1971).

TABLE I

Extended Basis Set of Slater Functions for HeO^+

Oxygen-Centered Functions

	1s	1s'	2s	2s'	2s"
1s (ζ = 13.324)[a]	0.03814	-0.00310	-	-	-
1s (ζ = 7.616)[a]	0.93888	-0.23613	-	-	-
2s (ζ = 5.944)[a]	0.04195	-0.15728	-	-	-
2s (ζ = 4.283)[a]	-	-	1.0	-	-
2s (ζ = 2.562)[a]	-	-	-	1.0	-
2s (ζ = 1.758)[a]	-	-	-	-	1.0
	2p	2p'	2p"		
2p (ζ = 8.450)[b]	0.01278	-	-		
2p (ζ = 3.744)[b]	0.25334	-	-		
2p (ζ = 2.121)[b]	-	1.0	-		
2p (ζ = 1.318)[b]	-	-	1.0		
	3d				
3d (ζ = 2.0)[c]	1.0				

Helium-Centered Functions

	1s	1s'	1s"
1s (ζ = 2.906)[b]	1.0	-	-
1s (ζ = 1.453)[b]	-	1.0	-
1s (ζ = 0.9)[c]	-	-	1.0
	2p	2p'	
2p (ζ = 3.0)[c]	1.0	-	
2p (ζ = 1.5)[c]	-	1.0	

TABLE I - References

[a] Functions taken from E. Clementi, Tables of Atomic Functions, a supplement to IBM J. Res. Develop. 9, 2 (1965).

[b] Functions taken from P. S. Bagus and T. L. Gilbert, Argonne National Laboratory Report ANL-7271, January 1968.

[c] Functions chosen in the present work.

TABLE II

Configurations Included in the First-Order Wavefunction of $^4\Sigma^-$ HeO$^+$

Excitation	Number of Occupancies	Number of $^4\Sigma^-$ Configurations
$1\sigma^2 2\sigma^2 3\sigma^2 4\sigma 1\pi^2$	1	1
$4\sigma \rightarrow n\sigma$ (n = 5,...,14)	10	10
$i\sigma \rightarrow 4\sigma$ (i = 1,2,3)	3	3
$\rightarrow n\sigma$	30	90
$1\pi \rightarrow m\pi$ (m = 2,...,6)	5	5
$j\sigma^2 \rightarrow 4\sigma n\sigma$ (j = 2,3)	20	20
$1\pi m\pi$	10	10
$2\sigma 3\sigma \rightarrow 4\sigma n\sigma$	10	30
$\rightarrow 1\pi m\pi$	5	20
$j\sigma 4\sigma \rightarrow 1\pi m\pi$	10	10
$j\sigma 1\sigma \rightarrow 4\sigma m\pi$	10	10
		209

TABLE III

Calculated Energies for the $^4\Sigma^-$, $^2\Pi$, and $^4\Pi$ States of HeO^+

R(Bohrs)	$^4\Sigma^-$	$^2\Pi$	$^4\Pi$
1.5	-76.60552	-76.99118	-76.32981
2	-77.04583	-77.1275	-76.71622
2.25	-77.14154	-77.13933	-76.78539
2.5	-77.19701	-77.13964	-76.81741
3	-77.24736	-77.13133	-76.83405
3.5	-77.26323	-77.12921	-76.83357
4	-77.26759	-77.12968	-76.83260
5	-77.26833	-77.12938	-76.83214

FIGURE CAPTIONS

FIGURE 1: Potential curves arising from the valence states of He and O^+, and He^+ and O, shifted vertically so as to match the known atomic energy levels at infinite separation. The dashed cruves are the results of the more accurate calculations, as discussed in Section IIA.

FIGURE 2: The inelastic cross section for $He + O^+(^4S) \rightarrow He + O^+(^2D)$, as a function of initial collision energy. The method of calculation is described in Section III.

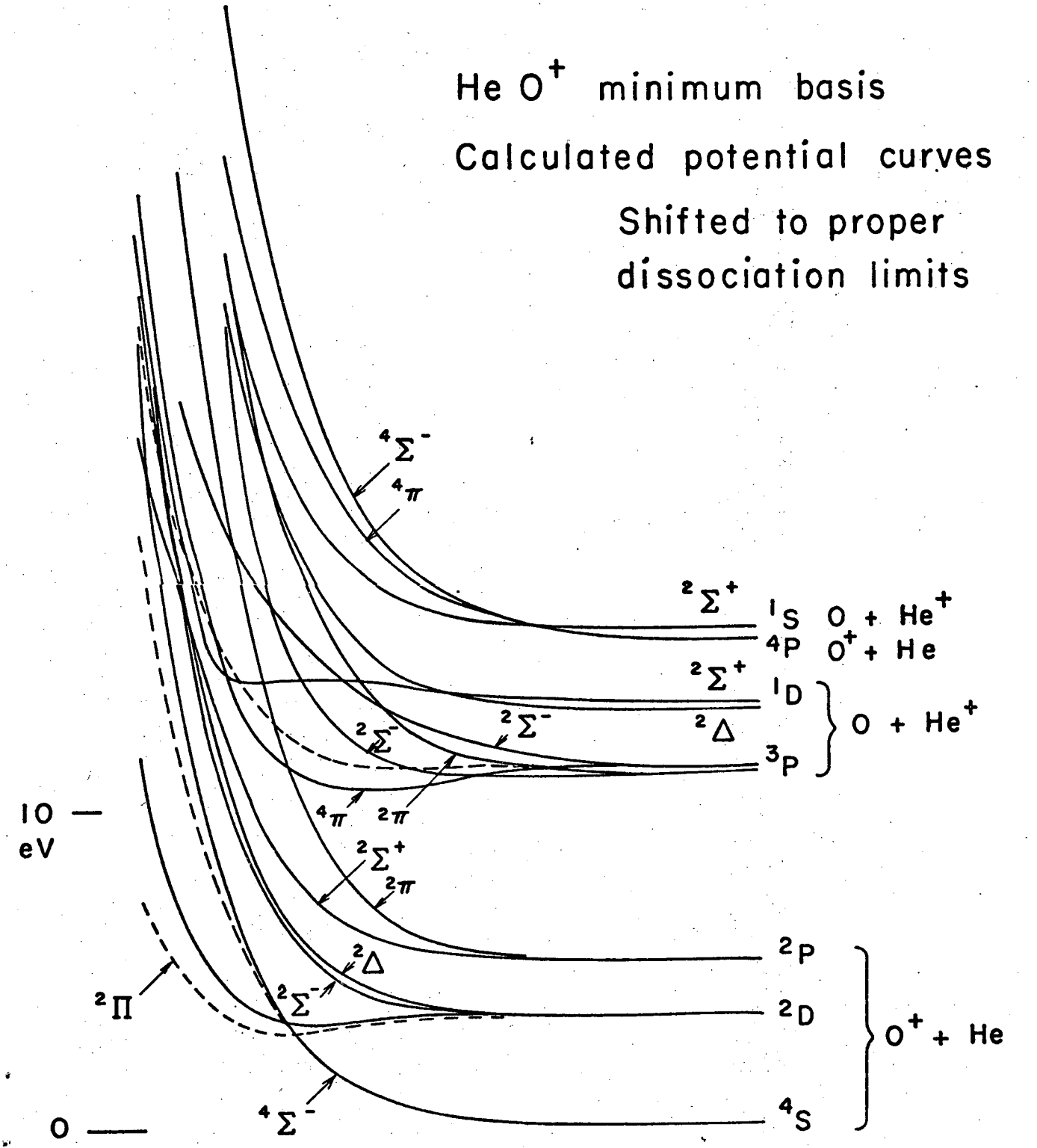

XBL7210-4234

Fig. 1

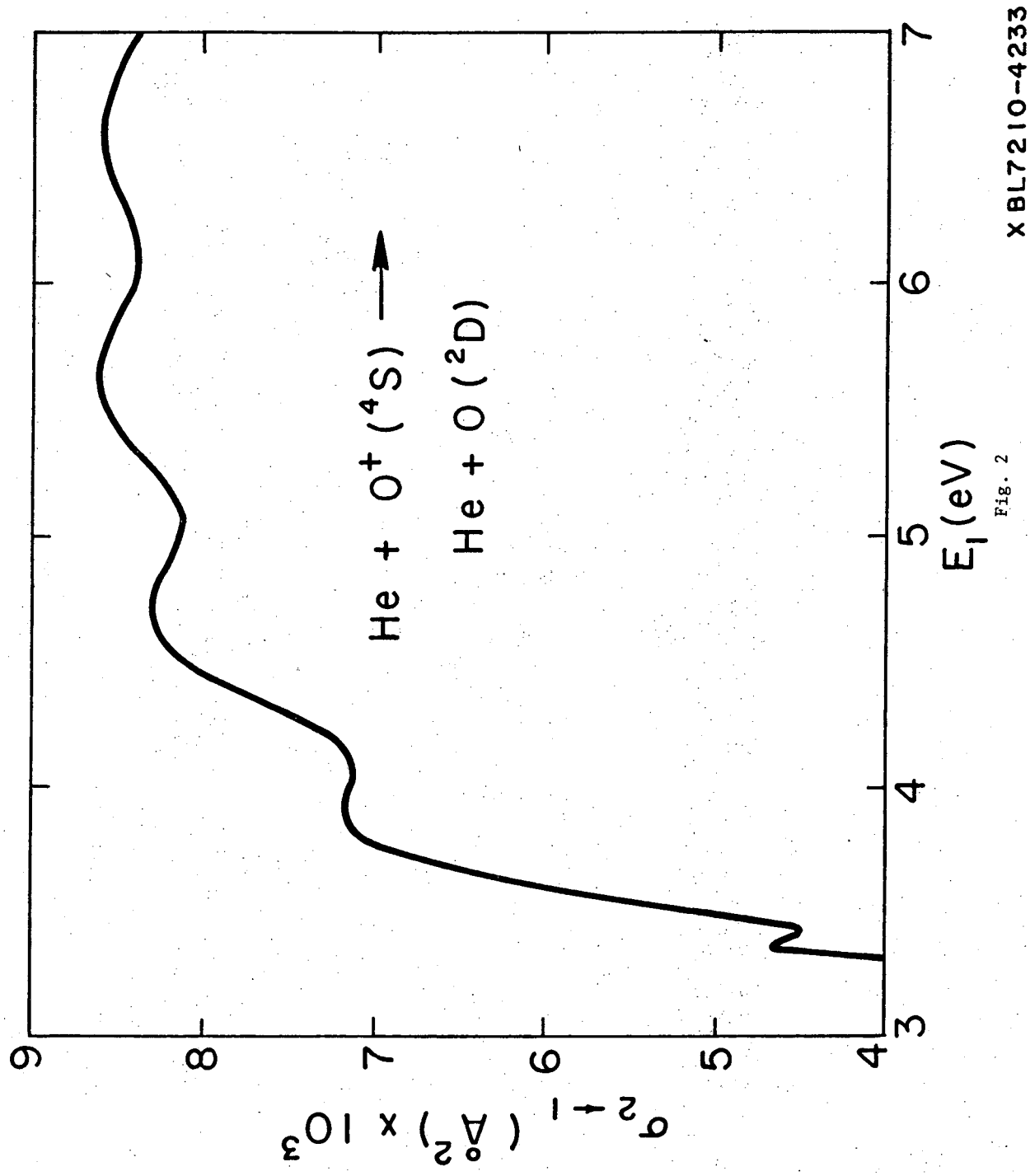

X BL7210-4233

Fig. 2

TECHNICAL INFORMATION DIVISION
LAWRENCE BERKELEY LABORATORY
UNIVERSITY OF CALIFORNIA
BERKELEY, CALIFORNIA 94720